

Submit to *International Journal of Thermophysics*

Study on Thermodynamic Properties of 1,1,1,2,3,3,3-Heptafluoropropane¹

Y. Y. Duan², L. Shi², M. S. Zhu^{2,3}, L. Z. Han², C. Zhang^{2,4}

¹ Paper presented at the Fourteenth Symposium on Thermophysical Properties, June 25-30, 2000, Boulder, Colorado, U.S.A.

² Department of Thermal Engineering, Tsinghua University, Beijing 100084, P.R. China.

³ To whom correspondence should be addressed.

⁴ Visiting Scholar from Department of Mechanical Engineering, Wuhan Institute of Science and Technology, Wuhan 430073, Hubei Province, P.R. China.

ABSTRACT

The vapor pressure of 1,1,1,2,3,3,3-heptafluoropropane (HFC-227ea) was measured in the temperature range from 243 to 375 K, and a vapor pressure equation for HFC-227ea was developed, from which the boiling point of HFC-227ea was determined. The pressure-volume-temperature (PVT) properties of HFC-227ea in gaseous phase were measured using Burnett/isochoric methods in the temperature range from 283 to 377 K and pressure range from 0.26 to 2.5 MPa. The maximum uncertainties for temperature and pressure in this work were estimated to be within ± 10 mK and ± 500 Pa, respectively. Based on the experimental data, a vapor pressure equation of HFC-227ea was developed, the virial coefficients, the saturated vapor density and the enthalpy of vaporization for HFC-227ea were also determined. The speed of sound of gaseous HFC-227ea was measured with a cylindrical, variable-path acoustic interferometer operating at 156.252 kHz, and then the ideal-gas heat capacity and second acoustic virial coefficient were calculated. A correlation of the second virial coefficient for HFC-227ea was obtained by a semi-empirical method using the square-well potential for the intermolecular force and was compared with the result based on PVT measurements. The surface tension of HFC-227ea was measured by differential capillary rise method (DCRM), seventy-eight data points were obtained in the temperature range from 243 to 340 K. The accuracy of the surface tension measurements was estimated to be within ± 0.15 mN·m⁻¹. Based on the experimental data, a van de Waals type surface tension correlation was proposed.

KEY WORDS: 1,1,1,2,3,3,3-heptafluoropropane; enthalpy of vaporization; HFC-227ea; PVT properties; speed of sound; surface tension; vapor pressure; virial coefficients

1. INTRODUCTION

The expected worldwide ban on many low-molar-mass chlorofluorocarbons has prompted a vigorous search for alternatives with zero ozone-depletion potential (ODP) and lower global warming potential (GWP). 1,1,1,2,3,3,3-heptafluoropropane (HFC-227ea) has zero ODP. It is a recently introduced, commercially available hydrofluorocarbon (HFC) useful in fire suppression, refrigeration, sterilization and propellant applications. It can be used as an alternative to halon, and blends containing HFC-227ea are potential alternatives to HCFC-22 and R502. Effective use of HFC-227ea requires that the thermodynamic and transport properties be accurately measured, but there is very little data available. Wirbser et al. [1] measured the specific heat capacity and Joule-Thomson coefficient of HFC-227ea; Salvi-Narkhede et al. [2] measured the vapor pressure, liquid molar volumes and critical properties; Park [3] measured the gaseous PVT properties with a Burnett apparatus at five temperatures; Klomfar et al. [4] measured the liquid PVT properties; Robin [5] listed the thermophysical properties of HFC-227ea including estimated transport properties; Defibaugh and Moldover [6] measured the liquid PVT behavior and the saturated liquid density; Weber [7] measured the vapor pressure of HFC-227ea; Laesecke and Hafer [8] measured the viscosity of HFC-227ea with a coiled capillary viscometer at low temperature and a straight capillary viscometer at high temperature; Pátek et al. [9] measured PVT properties of HFC-227ea with a Burnett apparatus at temperatures of 393 K and 423 K; Liu et al. [10, 11] measured the saturated liquid viscosity and gaseous thermal conductivity.

This paper reports the experimental results of vapor pressure, gaseous PVT property, speed of sound and surface tension of HFC-227ea. Based upon these data and results of literature, a vapor pressure equation, a virial equation of state and a van der Waals-type correlation of surface tension for HFC-227ea were developed; the virial coefficients, the ideal-gas heat capacity at constant pressure, the saturated vapor density and the enthalpy of

vaporization for HFC-227ea were also determined.

The sample of HFC-227ea was obtained from Shanghai Huiyou Chemical Corp., China and was used without further purification. The manufacturer stated that the water content was less than 20ppm. For the gas chromatographic analysis, the purity of the sample was better than 99.9 mol %.

2. VAPOR PRESSURE

Eighty-four vapor pressure data of HFC-227ea were measured over the temperature range from 243 to 375 K and corresponding pressure from 54 to 2936 kPa [12] and were shown in Fig. 1. The uncertainties of temperatures and pressures were ± 10 mK and ± 500 Pa, respectively. Independent duplicate measurements were made to avoid occasional error.

Based on the present vapor pressure measurements, a vapor pressure correlation, using a Wagner type function form, with the aid of the least-squares fitting, was developed as:

$$\ln(p / p_c) = (A_1\tau + A_2\tau^{1.25} + A_3\tau^3 + A_4\tau^7)T_c / T \quad (1)$$

where $\tau = 1 - T / T_c$, $A_1 = -8.095342$, $A_2 = 1.501634$, $A_3 = -3.099728$, $A_4 = -4.709418$, $T_c = 375.95$ K [6] is critical temperature and $p_c = 2987.74$ kPa is critical pressure which was determined by extrapolation of the experimental vapor pressure data to the critical temperature. The equation is valid for temperatures from 243 K to critical point. The temperature of normal boiling point is calculated to be $T_b = 256.708 \pm 0.010$ K.

The deviations of our experimental data, as well of literature data from Eq. (1) are shown in Fig. 2. The maximum absolute deviation of our data from Eq. (1) is 1.76 kPa, and the maximum relative deviation and root-mean-square (RMS) deviation are 0.12% and 0.047%, respectively. Fig. 2 shows that Weber's results [7] are systematically 0.2% higher than Eq. (1) and our data. The maximum and RMS deviation of Weber's results from Eq.

(1) are 0.23% and 0.18%, respectively. The experimental data of Salvi-Narkhede et al. [2] also exhibit systematic differences from our results. These data are about 7 kPa higher than our data in the temperature range from 305 K to critical point, about 2 kPa higher from 275 to 298 K and about 0.6 kPa lower from 243 to 268 K. The correlations of Salvi-Narkhede et al. [2] and Robin [5] were based on the experimental data of Salvi-Narkhede et al. [2], so their curves also show the similar systematic differences from Eq. (1). We don't know the reasons for the apparent systematic errors.

3. PVT PROPERTY, VIRIAL COEFFICIENTS AND EQUATION OF STATE

One hundred and forty one pressure-volume-temperature data points for HFC-227ea in the gaseous phase have been measured using Burnett/isochoric methods and shown in Fig. 1. Burnett expansion measurements were made both at 363.15 K and at 318.15 K. Based on the pressure-density relationships established at 363.15 K and 318.15 K, data were collected along 9 isochores for temperatures from 283 to 377 K, pressures from 0.26 to 2.5 MPa. The maximum temperature uncertainty and maximum pressure uncertainty in this work were estimated to be within ± 10 mK and ± 500 Pa, respectively [13]. Along each isotherm, the second and third virial coefficients of HFC-227ea were extrapolated from the gaseous PVT measurements and listed in Table I. The present second and third virial coefficients of HFC-227ea along with the results of Pátek et al. [9] were correlated as follows:

$$B / \text{dm}^3 \cdot \text{mol}^{-1} = B_0 + B_1 T_r^{-1} + B_2 T_r^{-2} + B_3 T_r^{-3} + B_4 T_r^{-6} + B_5 T_r^{-8} \quad (2)$$

$$C / \text{dm}^6 \cdot \text{mol}^{-2} = C_0 + C_1 T_r^{-\frac{1}{2}} + C_2 T_r^{-1} + C_3 T_r^{-2} \quad (3)$$

where B and C are second and third virial coefficients, respectively, $T_r = T / T_c$, $T_c = 375.95$ K [6] is critical temperature, the coefficients B_1 to B_5 and C_0 to C_3 were determined by fitting Eqs. (2) and (3) to the experimental data and listed in Table II.

Figures 3 and 4 show the comparisons of present data and literature results with Eqs.

(2) and (3) of second and third virial coefficients for HFC-227ea.. Based on Eqs. (2) and (3), a two-term virial equation were determined to represent the gaseous thermodynamic properties of HFC-227ea as follow

$$\frac{p}{\rho RT} = 1 + B\rho + C\rho^2 \quad (4)$$

where $R = 8.314471 \text{ J} \cdot \text{K}^{-1} \cdot \text{mol}^{-1}$ is universal gas constant, ρ is density. The suitable range of this equation is from 283 to 453 K in temperature and up to $2.5 \text{ mol} \cdot \text{dm}^{-3}$ in density in gaseous phase. Figure 5 shows the deviations of the experimental data of present work and literatures from Eq. (4). From the deviation plot, it is clear that Eq. (4) can represent our data and the results of Pátek et al. [9] very well, but Park's values [3] are 0.05 to 1.3% higher than Eq. (4).

4. SATURATED GASEOUS DENSITY AND ENTHALPY OF VAPORIZATION

The saturated vapor densities of HFC-227ea were extrapolated from the PVT measurements and Eq. (1) and correlated as follow:

$$\rho_r = 1 + b_1\tau^\beta + b_2\tau^{2\beta} + b_3\tau + b_4\tau^{1/\beta} \quad (5)$$

where $\rho_r = \rho / \rho_c$, $\rho_c = 580 \text{ kg} \cdot \text{m}^{-3}$ is the critical density [6], $\beta = 0.325$ is the critical exponent, $b_1 = -0.66473289$, $b_2 = -6.6731565$, $b_3 = 12.205996$ and $b_4 = -6.0067685$ are coefficients determined by fitting Eq. (3) to the data.

According to the Clapeyron equation, the enthalpy of vaporization can be determined from:

$$r = h'' - h' = \left(\frac{dp}{dT}\right)_\sigma T \left(\frac{1}{\rho''} - \frac{1}{\rho'}\right) \quad (6)$$

where r is the enthalpy of vaporization, $\left(\frac{dp}{dT}\right)_\sigma$ is the first derivative of the vapor pressure and can be calculated from Eq. (1), h'' and h' are the enthalpies of the

saturated vapor and liquid, respectively, and ρ'' and ρ' are the densities of the saturated vapor and liquid and can be calculated from Eq. (5) and saturated liquid density correlation provided by literature [6], respectively.

The enthalpy of vaporization of CF₃I was calculated from Eq. (5) and correlated by the following equation:

$$r / RT_c = b_0 \tau^\beta + b_1 \tau^{\beta+\Delta_1} + b_2 \tau^{1-\alpha+\beta} + \sum_{i=1}^3 a_i \tau^i \quad (7)$$

where $\tau = 1 - T / T_c$, $\alpha = 0.1085$, and $\beta = 0.325$ are the critical exponent, $\Delta_1 = 0.50$ is the first symmetric correlation-to-scaling exponent. The coefficients $b_0 = -9.65051$, $b_1 = 664.076$, $b_2 = 1091.13$, $a_1 = -1536.48$, $a_2 = -302.081$ and $a_3 = 129.274$ were determined by fitting Eq. (7) to the data calculated from Eq. (6).

5. SPEED OF SOUND

According to speed of sound data, the ideal-gas heat capacity at constant pressure and the virial coefficient can be derived. There are no available speed of sound data of HFC-227ea published before this study, and only one set of ideal-gas heat capacity data in the temperature range from 253 to 423 K extrapolated from specific heat capacity experimental results was reported by Wirbser et al. [1]. The speed of sound of gaseous HFC-227ea were measured at temperatures from 273 to 333 K and pressures from 26 to 315 kPa with a cylindrical, variable-path acoustic interferometer operating at 156.252 kHz. The speed of sound results of HFC-227ea were obtained from the corrected wavelengths together with the fixed frequency. Figure 6 shows the measured speed of sound results versus pressure along each isotherm. The uncertainty of the speed of sound measurements was less than $\pm 0.05\%$ [14].

According to thermodynamic relations, the ideal-gas heat capacity at constant pressure, C_p^0 , and second acoustic virial coefficient, β_a , can be determined using the

speed of sound results, C_p^0 and β_a data were correlated by the following equations:

$$C_p^0 / R = -0.54931 + 0.08772(T / K) - 1.10655 \times 10^{-4}(T / K)^2 \quad (8)$$

$$\beta_a (\text{cm}^3 \cdot \text{mol}^{-1}) = -6.19641 \times 10^3 + 25.24(T / K) - 0.02737(T / K)^2 \quad (9)$$

The maximum deviation of the measured ideal-gas heat capacity data from Eq. (8) was less than 0.5%. The results of Wirbser et al. [1] are higher than calculated values from Eq. (8) by about 1 to 6%. The maximum deviation of the second acoustic virial coefficient data from Eq. (9) is less than 2.5%.

Based on the measurements, the second virial coefficient, B , of HFC-227ea was obtained by a semi-empirical method using the square-well potential for the intermolecular force, and it was correlated as

$$B(\text{cm}^3 \cdot \text{mol}^{-1}) = 25.26\{1 - 3.142914[\exp(670.0/T) - 1]\} \quad (10)$$

The comparison of Eq. (10) with the data derived from PVT measurements and Eq. (2) are shown in Fig. 3.

6. SURFACE TENSION

Surface tension data for HFC-227ea have been measured with a differential capillary rise method (DCRM). The sample cell of the measurement system contained three capillaries with the following bore radii: $r_1 = 0.128 \pm 0.001 \text{ mm}$, $r_2 = 0.262 \pm 0.001 \text{ mm}$, and $r_3 = 0.385 \pm 0.002 \text{ mm}$. Measurements were conducted under equilibrium conditions between the liquid and its saturated vapor. Two data sets for a total of seventy-eight surface tension data for HFC-227ea were measured in the temperature range from 243 to 340 K using capillaries 1 and 2 and capillaries 1 and 3 [15]. The measurement uncertainties for surface tension and temperature are estimated to be within $\pm 0.15 \text{ mN} \cdot \text{m}^{-1}$ and $\pm 20 \text{ mK}$, respectively. The saturated vapor density of

HFC-227ea was calculated from Eq. (5) and the saturated liquid density came from literature [6]. A van de Waals type surface tension correlation was used to correlate the experimental data

$$\sigma = \sigma_0 (1 - T / T_c)^n \quad (11)$$

where σ is the surface tension, $\sigma_0 = 50.634 \text{ mN} \cdot \text{m}^{-1}$, and $n = 1.250$ as determined by a least-squares fit, $T_c = 375.95 \text{ K}$ is critical temperature[6]. Figure 7 shows the surface tension of HFC-227ea versus the temperature. The maximum absolute deviation of the experimental data from Eq. (11) are $\pm 0.14 \text{ mN} \cdot \text{m}^{-1}$, which is smaller than the estimated uncertainty $\pm 0.15 \text{ mN} \cdot \text{m}^{-1}$.

ACKNOWLEDGMENT

This work was supported by the National Natural Science Foundation of China (No. 59906006). We are grateful to Ms. Xia Lei for providing useful help in measurements.

REFERENCES

1. H. Wirbser, G. Bräuning, J. Gurtner, and G. Ernst, *J. Chem. Thermodyn.* **24**:761 (1992).
2. M. Salvi-Narkhede, B. H. Wang, J. L. Adcock, and W. A. Van Hook, *J. Chem. Thermodyn.* **24**:1065 (1992).
3. Y. J. Park, *Bestimmung des thermischen Verhaltens neuer Arbeitsstoffe der Energietechnik mit Hilfe einer Burnett-Apparatur*. Ph.D. Thesis, Universität Karlsruhe, (1993).
4. J. Klomfar, J. Hruby, and O. Sifner, *J. Chem. Thermodyn.* **26**:965 (1994).
5. M. L. Robin, In *Proc. International CFC and Halon Alternatives Conf.* (Washington, D.C., 1994), p.105.
6. D. R. Defibaugh and M. R. Moldover, *J. Chem. Eng. Data* **42**:650 (1997).
7. L. A. Weber, Personal Communication, (1998).
8. A. Laesecke and R. F. Hafer, *J. Chem. Eng. Data* **43**:84 (1998).
9. J. Pátek, J. Klomfar, J. Prazak, and O. Sifner, *J. Chem. Thermodyn.* **30**:1159 (1998).
10. X. J. Liu, L. Shi, M. S. Zhu, and L. Z. Han, *J. Chem. Eng. Data* **44**:688 (1999).
11. X. J. Liu, L. Shi, Y. Y. Duan, M. S. Zhu, and L. Z. Han, *J. Chem. Eng. Data* **44**:882 (1999).
12. L. Shi, Y. Y. Duan, M. S. Zhu, L. Z. Han, and X. Lei, *Fluid Phase Equil.* **163**:109 (1999).
13. L. Shi, Y. Y. Duan, M. S. Zhu, L. Z. Han, and X. Lei, *J. Chem. Eng. Data* **44**:1402 (1999).
14. C. Zhang, Y. Y. Duan, L. Shi, M. S. Zhu, and L. Z. Han, Submitted to *Fluid Phase Equil.*
15. Y. Y. Duan, L. Shi, M. S. Zhu, L. Z. Han, and X. Lei, Submitted to *Fluid Phase Equil.*

Table I. Second and third virial coefficients of HFC-227ea

$T(\text{K})$	$B(\text{dm}^3 \cdot \text{mol}^{-1})$	$C(\text{dm}^6 \cdot \text{mol}^{-2})$	$T(\text{K})$	$B(\text{dm}^3 \cdot \text{mol}^{-1})$	$C(\text{dm}^6 \cdot \text{mol}^{-2})$
377.15	0.3600	0.04508	328.15	0.5151	0.04947
373.15	0.3700	0.04571	323.15	0.5357	0.04736
368.15	0.3834	0.04705	318.15	0.5589	
363.15	0.3971	0.04770	313.15	0.5820	
358.15	0.4119	0.04915	308.15	0.6069	
353.15	0.4268	0.04932	303.15	0.6333	
348.15	0.4420	0.04894	298.15	0.6612	
343.15	0.4578	0.04749	293.15	0.6905	
338.15	0.4771	0.05108	288.15	0.7209	
333.15	0.4961	0.05157	283.15	0.7519	

Table II. Coefficients of Eqs. (2) and (3)

B_0	B_1	B_2	B_3	B_4	B_5
-19.466560	74.520374	-100.67156	49.097250	-4.6492370	0.80728384
C_0	C_1	C_2	C_3		
10.553229	-28.752602	22.022480	-3.7780755		

Captions to figures

Fig. 1. Distribution of PVT and vapor pressure measurements for HFC-227ea. (\square) vapor pressure data; (—) calculation from vapor pressure equation; (\blacksquare) critical point; (\diamond) Burnett measurements; (Δ) isochoric measurements.

Fig. 2. Deviations of the vapor pressure data from Eq. (1). (\blacksquare) this work; (\square) Weber [7]; (Δ) Salvi-Narkhede et al. [2]; (—) correlation of Salvi-Narkhede et al. [2]; (— — —) correlation of Robin[5].

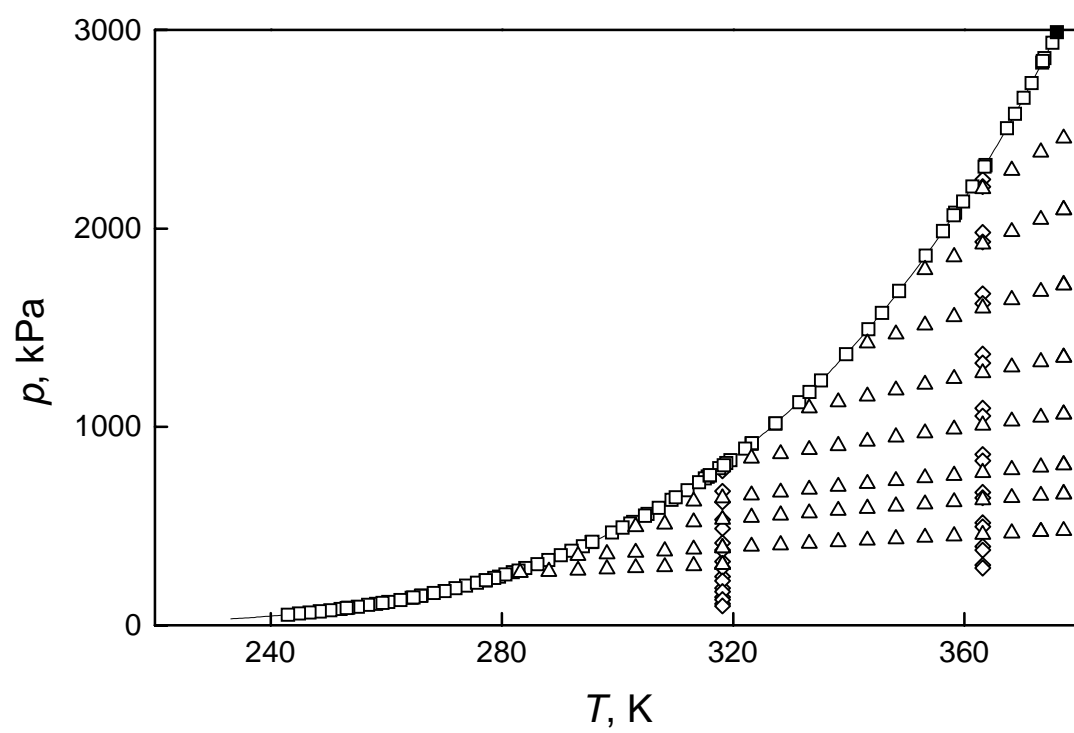
Fig. 3. The second virial coefficient of HFC-227ea versus temperature. (\square) this work; (\diamond) Park [3]; (Δ) Pátek et al. [9]; (—) Eq. (2); (- - -) Eq. (10).

Fig. 4. The third virial coefficients of HFC-227ea versus temperature. (\square) this work; (\diamond) Park [3]; (Δ) Pátek et al. [9]; (—) Eq. (3).

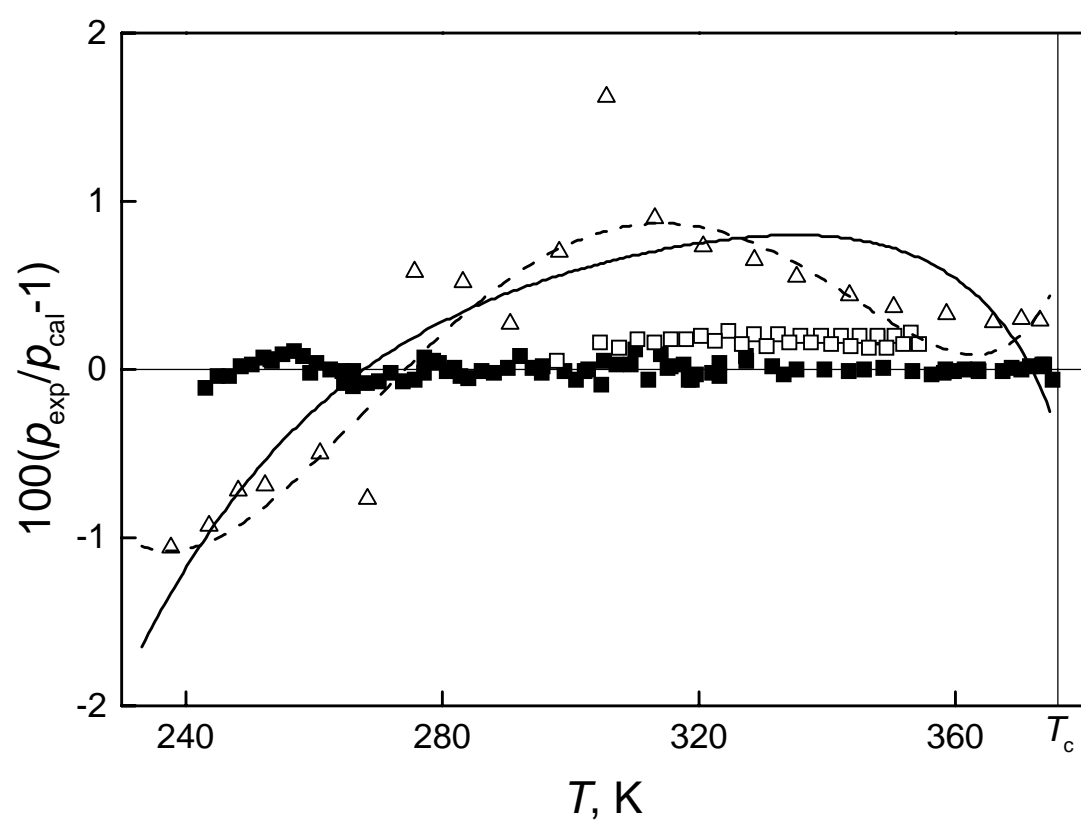
Fig. 5. Pressure deviations of measured PVT data for HFC-227ea from values calculated using Eq (5). (\square) this work; (\diamond) Park [3]; (Δ) Pátek et al. [9].

Fig. 6. Experimental speed of sound data for HFC-227ea.

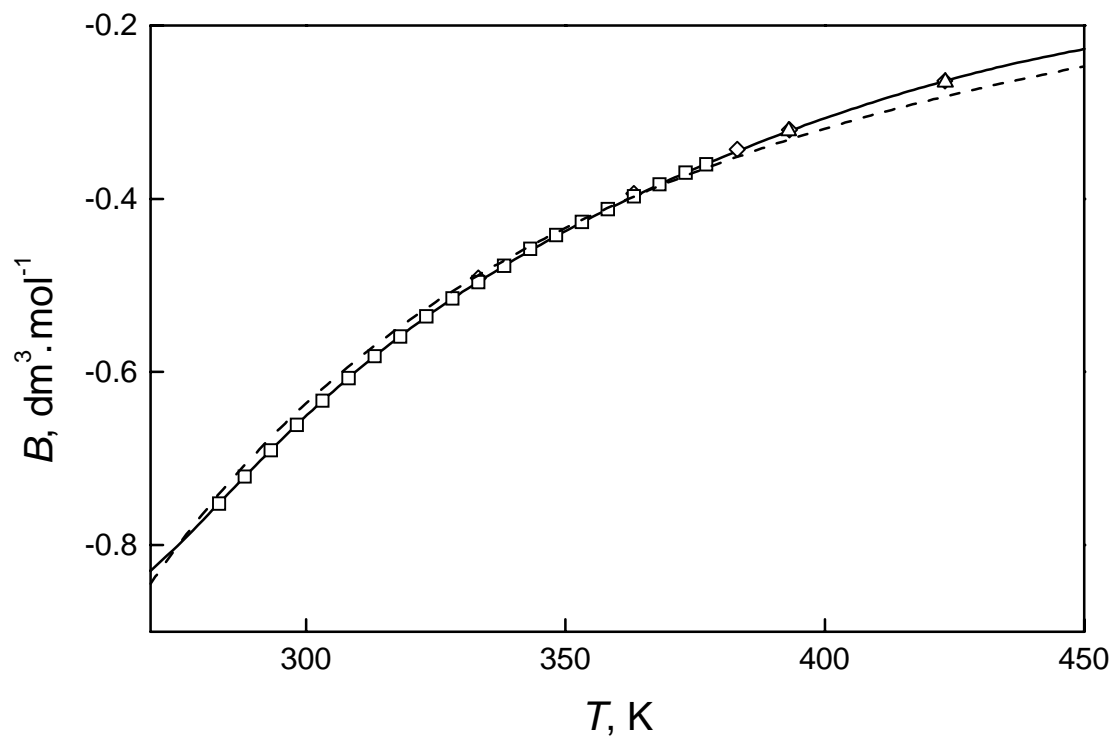
Fig. 7. Surface tension versus temperature for HFC-227ea: (\square)1,2; (Δ)1,3.



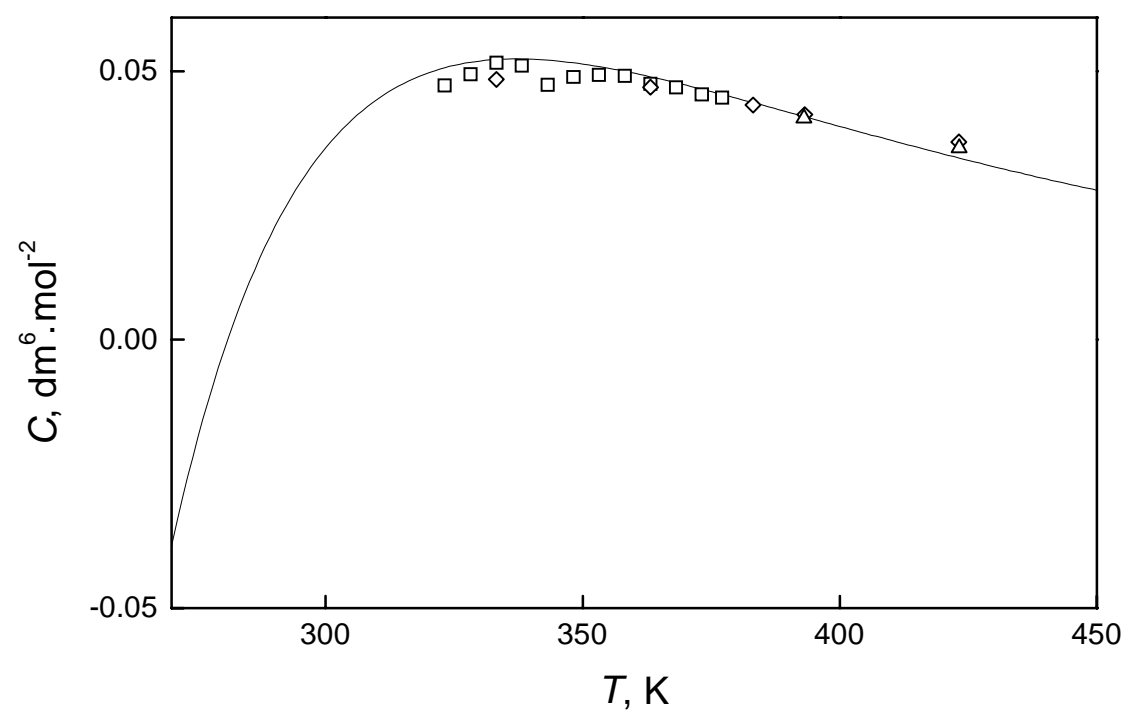
Duan et al. **Fig. 1.**



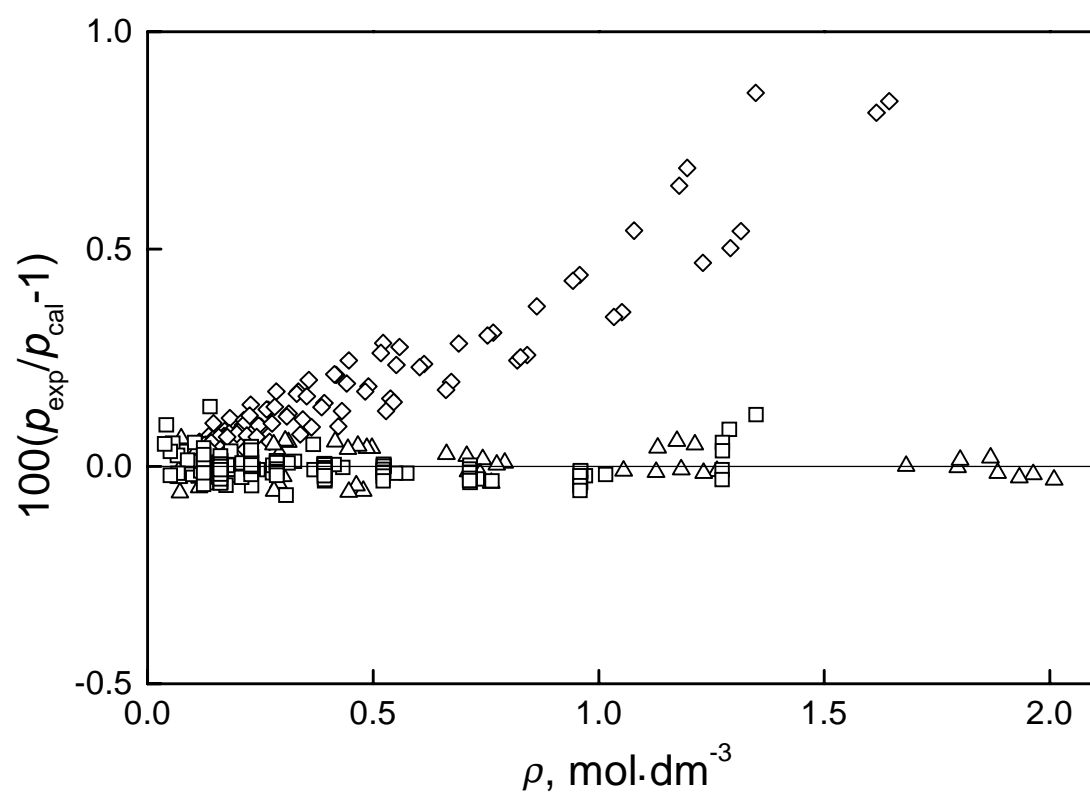
Duan et al. **Fig. 2.**



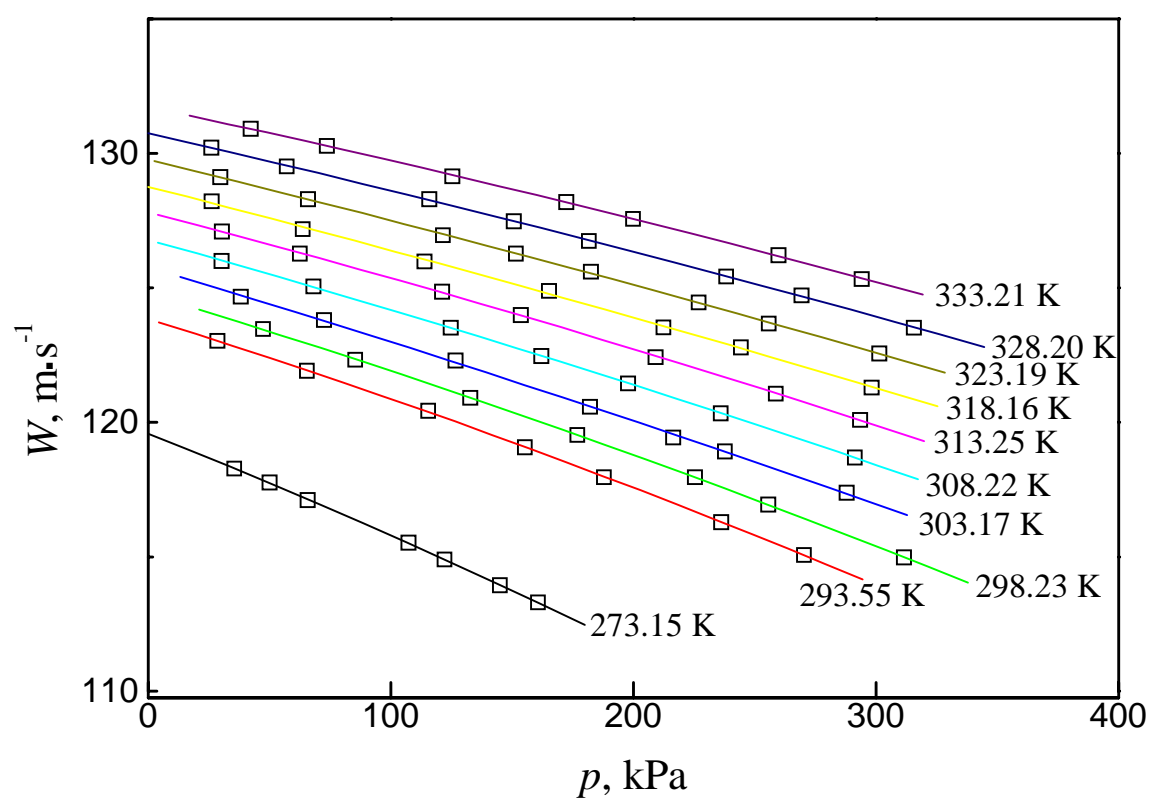
Duan et al. **Fig. 3.**



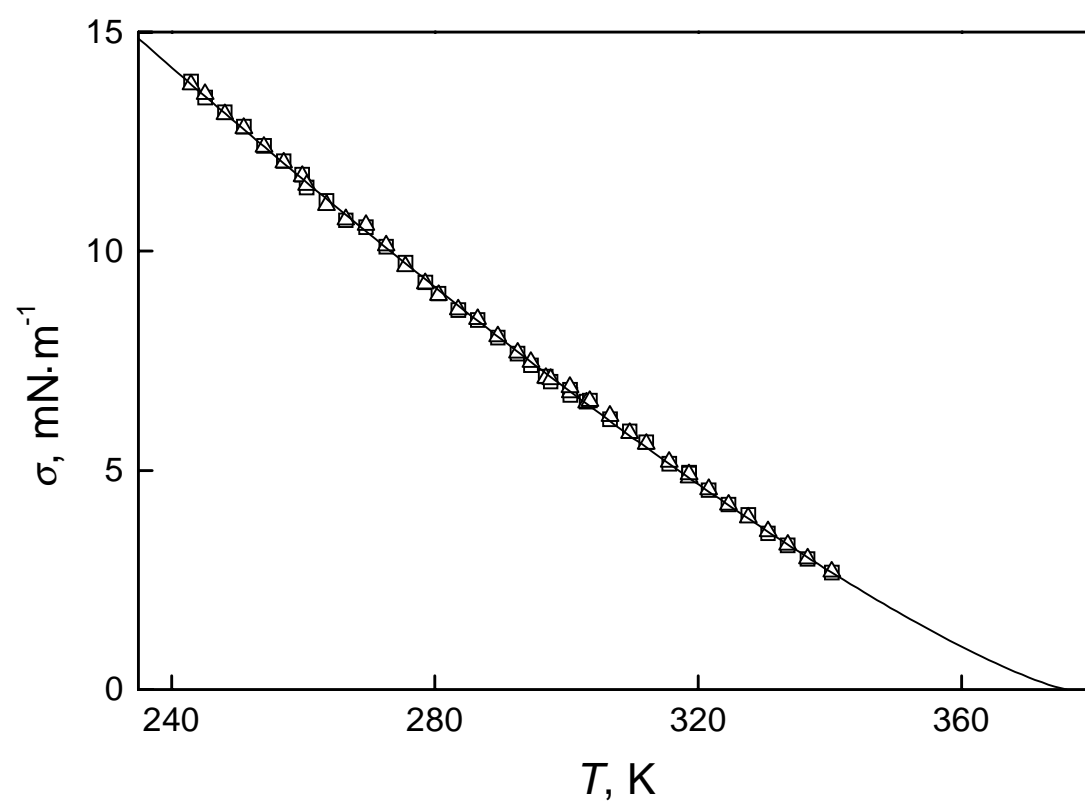
Duan et al. **Fig. 4.**



Duan et al. **Fig. 5.**



Duan et al. **Fig. 6.**



Duan et al. **Fig. 7.**